Fuzzy "Along" Spatial Relation in 3D. Application to Anatomical Structures in Maxillofacial CBCT

Timothée Evain[1,2(✉)], Xavier Ripoche[2], Jamal Atif[3], and Isabelle Bloch[1]

[1] Institut Mines Télécom, Télécom ParisTech, CNRS LTCI, Paris, France
tevain@telecom-paristech.fr
[2] Carestream Dental, Croissy-Beaubourg, France
[3] PSL, LAMSADE CNRS UMR 7243, Université Paris-Dauphine, Paris, France

Abstract. Spatial relations have proved to be of great importance in computer vision and image understanding. One issue is their modeling in the image domain, hence allowing for their integration in segmentation and recognition algorithms. In this paper, we focus on the "along" spatial relation. Based on a previous work in 2D, we propose extensions to 3D. Starting from the inter-objects region, we demonstrate that the elongation of the interface between the objects and this region gives a good evaluation of the alongness degree. We also integrate distance information to take into account only close objects parts. Then we describe how to define the alongness relation within the fuzzy set theory. Our method gives a quantitative satisfaction degree of the relation, reliable for differentiating spatial situations. An original example on the maxillofacial area in Cone-Beam Computed Tomography (CBCT) illustrates how the proposed approach could be used to recognize elongated structures.

Keywords: Spatial relations · Fuzzy reasoning · Dental imaging

1 Introduction

Spatial relations have proved to be of great importance in numerous fields such as psychology, cartography, linguistics, and computer science [4,8,9]. They are a major concept in human reasoning for object perception, recognition, or mutual comprehension [1]. In computer vision and image understanding, spatial relations carry reliable information [6,11,15]. Many relations have been investigated in the literature [2], and several applications have been proposed, for example in brain segmentation [5]. However, while extension to 3D of simple relations is straightforward, there is still work to do for complex relations.

The alongness relation is one of these complex relations, yet important. For example, in dental practice, "along" is usually used to describe the position of the mandibular canal with respect to the mandible. Since this canal contains the very sensitive mental nerve, to avoid severe patient injury during surgery, such as dysesthetia or neuropathic pain, dental surgeons have to identify its position.

V. Murino and E. Puppo (Eds.): ICIAP 2015, Part I, LNCS 9279, pp. 271–281, 2015.
DOI: 10.1007/978-3-319-23231-7_25

This type of relation is intrinsically vague and its definition can benefit from fuzzy set based modeling [2,7]. To the best of our knowledge, only few works in the literature have addressed the modeling of this relation [13,14]. In [13], in the context of geographic information systems, the alongness is computed between a line and an object. The relation is defined as the intersection length between the line and a buffer zone around the object boundary, normalized by the length of the boundary or the length of the line. In [14], the relation is considered as an alongness degree. It is defined as the length of objects boundaries in contact with the inter-objects region, normalized by the area of this region. A way to introduce distance information is also shown, as well as methods to deal with fuzzy objects. In this paper we propose to extend this approach to deal with 3D (and possibly fuzzy) objects.

In Section 2 we present the general approach to define the along relation, which is based on inter-objects region described in Section 3 and an elongation measure, that we introduce in Section 4. The extension to fuzzy sets is then presented in Section 5. Results are discussed in Section 6.

2 General Approach to Define "Along"

In this work, we consider that two objects A and B are related by an "along" relation if at least one of them is elongated and A and B are side by side in the direction of elongation. "Side by side" implicitly means that the two objects are close to each other comparatively to their environment. Such conditions imply a specific shape for the space between A and B which should be elongated. The measure of elongation of the region between the objects can therefore be used to define the along relation, as suggested in [14].

This approach requires a definition of "betweenness" to model the inter-objects space. Another advantage is that the relation is symmetrical, considering both objects equivalently, and gives the possibility to have a satisfaction degree and not just a binary one, as already argued in [7]. Looking at the inter-objects region allows us also to compute the relation only between parts of objects, based on the distance between them. The global method to define alongness is then:

1. Compute the inter-objects region β.
2. Define the elongation of β.
3. Compute the degree of satisfaction of the relation.

3 Inter-Objects Region

Several methods exist for computing the region β between two compact objects A and B [3]. We focus on the "visibility" method [3] which is able to deal with difficult situations like concavities. It is based on admissible segments. A segment $]a, b[$ is said admissible if a and b are in A and B respectively, and if the segment is included in $A^C \cap B^C$, where the superscript C denotes the complement of the

object (note that this forces a and b to be on the boundaries of objects). The region β can then be defined as:

$$\beta(A,B) = \cup\{\ ]a,b[\ \mid a \in A, b \in B,\ ]a,b[\ \subseteq\ A^C \cap B^C\}$$

This definition does not make any assumption on the space dimensionality, and can be used directly in 3D. The two main limitations of this approach are when one of the objects is much more extended than the other one (see [3] for a definition dealing with such cases), and when the alongness relation is computed between sets of disconnected objects. These cases will not be investigated in this paper.

4 Elongation Measure

4.1 Common Definition

One common definition of elongation is to consider the inverse of compactness [10] as:

$$e_{3\mathrm{D}}(\beta) = \frac{S^3(\beta)}{V^2(\beta)}$$

with S and V the area and volume of β, respectively. This definition is dimensionless, admits a minimum equal to 36π for spherical shapes, and increases for more elongated shapes. This definition is a good start since the measure is invariant by translation, rotation and isotropic scaling. We can now define the elongation degree as $\alpha_1 = f_a\left(e_{3\mathrm{D}}(\beta)\right)$ where f_a is an increasing function, e.g. $\frac{1-e^{-ax}}{1+e^{-ax}}$, with $\alpha \in [0,1]$. Normalizing the degree is important to compare different degrees with various ranges. Another way to define the degree is to normalize e_{3D} by the value for a sphere. The degree is then in $[1,+\infty[$.

4.2 Alongness Degree Based on Object Boundaries

The region β could however be elongated without A and B being along each other. An additional constraint is that β is elongated in the direction of A and B, which relies on the contact surface between $A \cup B$ and β [14]. However, in 3D, if we just consider the total area of β in contact with the objects, it is impossible to distinguish between two rectangular cuboids whose longest sides are facing each other (Figure 1 (a) first case) and two cylinders whose bases are facing each other (Figure 1 (a) second case) if the total areas of facing surfaces are equal for example.

Therefore in 3D, the inter-objects region should be elongated in only one direction. We propose the following new definition to include this constraint:

$$\alpha_2 = f_a\left(\frac{(\gamma_A S_A^c(\beta) + \gamma_B S_B^c(\beta))^3}{V(\beta)^2}\right) \qquad \text{with} \qquad \gamma_X = 1 - \frac{2\sqrt{S_X^c(\beta)\pi}}{P_X^c(\beta)} \tag{1}$$

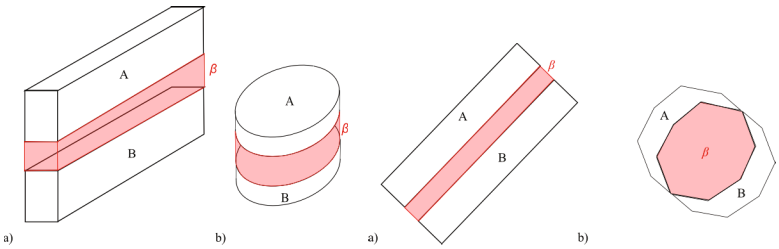

(a) Considering only interface area lead to ambiguities

(b) Distance is needed to distinguish the two configurations.

Fig. 1. Configurations possibly leading to the same elongation degree.

where $S_X^c(\beta)$ is the frontier area between β and the object X, and $P_X^c(\beta)$ the perimeter of this surface boundaries. γ_X is a measure of the elongatedness of the contact surface. When it tends to a circular shape, γ_X will tend to zero as the ratio will tend to 1 (equal to 1 in a perfect flat circle case, which is the less elongated possible shape), and increases toward 1 if the shape is more elongated, as the ratio will tend to zero. This definition takes into account the shape of both objects separately.

4.3 Including Distance Information

In some situations such as the one depicted in Figure 1 (b), the distance between the two objects can be meaningful: first configuration is closer to the intuitive "along" relation than the second one, but the α_2 score will not differentiate these two cases if the area and the volume of β are the same.

As in [14], we use the function $D_{AB}(x)$ to include distance:

$$\nu(\beta) = \int_\beta D_{AB}(x)dx \quad \text{with} \quad D_{AB}(x) = d(x, A) + d(x, B) \tag{2}$$

where $d(x, A)$ and $d(x, B)$ are the distances from x to A and B respectively, and ν is the β hyper-volume.

We can now define a new measure which includes this distance information as:

$$\alpha_3 = f_a\left(\frac{(\gamma_A S_A^c(\beta) + \gamma_B S_B^c(\beta))^2}{\nu(\beta)}\right) \tag{3}$$

One can note that exponents have changed to keep the degree dimensionless. One drawback of this degree is the loss of invariance to isotropic scaling since the distance involved in the definition is not normalized. This invariance could be obtained by normalizing the distance by its maximum value.

4.4 Using Distance to Take into Account Only Close Parts

We can examine the spatial relation only on parts of objects which are close to each other, which may be useful depending on object shapes (e.g. if two coils are next to one another, it is possible to tell if they are twisted in the same orientation or not). We reduce β by thresholding it at a distance t to keep only points which have a lower distance value, leading to β_t. This threshold can create holes so consistency should be ensured by either filling holes in each connected component of β_t or by looking for an optimal threshold around the initial one which gives only non hollow connected components when they exist. The degrees α_4 and α_5 are then defined by replacing β by β_t in (1) and (3).

5 Extension to Fuzzy Objects

The inclusion of the segment in the complement of the fuzzy objects is now modeled as a degree of inclusion [2] which can be expressed as:

$$\mu_{\text{inc}}(]a,b[) = \inf_{x\in]a,b[} \min[1-\mu_A(x), 1-\mu_B(x)]$$

where μ_A and μ_B are the membership functions of the two fuzzy sets (we identify in this paper a fuzzy set with its membership function, to simplify notations). Now β is the fuzzy set defined by [14]:

$$\mu_\beta(x) = \sup\{\mu_{inc}(]a,b[) \mid a \in \text{Supp}(\mu_A), b \in \text{Supp}(\mu_B), x \in]a,b[\}$$

This definition implies that the degree is equal to 1 when the segment is fully visible and equal to 0 if at least one of its points is not visible.

For a 3D fuzzy set μ, area and volume are defined as integrals of the gradient magnitude and their membership function as:

$$S(\mu) = \int_{\text{Supp}(\mu)} |\nabla\mu(x)|dx \qquad V(\mu) = \int_{\text{Supp}(\mu)} \mu(x)dx$$

which are direct extensions of definitions in [12]. To define the surface where the β region and an object μ are in contact, we now take the intersection of the support of the object and β. The frontier is then:

$$F_\mu = (\ \text{Supp}(\mu) \cap \text{Supp}(\mu_\beta)\ ) \quad \text{leading to} \quad S^c_\mu = \int_{F_\mu} |\nabla\mu(x)|dx \tag{4}$$

Equation (1) becomes:

$$F\alpha_2 = f_a\left(\frac{(S^c_{\mu_A}(\mu_\beta) + S^c_{\mu_B}(\mu_\beta))^3}{V(\mu_\beta)^2}\right) \tag{5}$$

To add the distance information, we propose to consider the minimal length between the supports of each point rather than the length of admissible segments [14] as:

$$D_{\mu_A\mu_B}(x) = \inf\{||\overrightarrow{ab}|| \mid a \in \text{Supp}(\mu_A), b \in \text{Supp}(\mu_B), x \in]a,b[\}$$

Equation (2) is then modified by weighting $D_{\mu_A\mu_B}(x)$ by $\mu_\beta(x)$ [14]:

$$\nu(\mu_\beta) = \int_{\text{Supp}(\mu_\beta)} \mu_\beta(x) D_{\mu_A\mu_B}(x)\ dx \tag{6}$$

A degree $F\alpha_3$ is defined by replacing the volume in (5) by (6). Using a distance threshold as suggested for α_4 and α_5 would result in a loss of the fuzzy nature of the area, so to avoid this, we use a decreasing function $g : \mathbb{R} \longrightarrow [0, 1]$ of $D_{\mu_A\mu_B}$. β_t becomes a fuzzy set:

$$\mu_{\beta_t}(x) = \mu_\beta(x) g(D_{\mu_A\mu_B}(x)) = \mu_\beta(x)(1 - f_{a_1}(D_{\mu_A\mu_B}(x)))$$

where f_{a_1} is the same kind of function as f_a, i.e. a normalizing function. In order to obtain the frontier of β_t, one can simply replace β by β_t in (4). To define $F\alpha_4$ and $F\alpha_5$, β is replaced by β_t in $F\alpha_2$ and $F\alpha_3$ respectively. Table 1 summarizes the proposed definition.

Table 1. Summary of proposed degrees.

Degree	Formula	Description
α_1	$f_a\left(\frac{S^3(\beta)}{V^2(\beta)}\right)$	Inverse of compactness. Ranges from 0 for spherical shapes and tends towards 1 for vessel-like shapes
α_2	$f_a\left(\frac{(\gamma_A S_A^c(\beta)+\gamma_B S_B^c(\beta))^3}{V(\beta)^2}\right)$	Ratio taking into account only interface areas between β and the objects. The areas are weighted by an elongation score favoring elongated interfaces.
α_3	$f_a\left(\frac{(\gamma_A S_A^c(\beta)+\gamma_B S_B^c(\beta))^2}{\nu(\beta)}\right)$	Same as α_2 but the volume is weighted by the absolute minimal distance to the objects.
α_4	$f_a\left(\frac{(\gamma_A S_A^c(\beta_t)+\gamma_B S_B^c(\beta_t))^3}{V(\beta_t)^2}\right)$	Same as α_2 with a thresholded β on the distance to take into account only close parts of objects.
α_5	$f_a\left(\frac{(\gamma_A S_A^c(\beta_t)+\gamma_B S_B^c(\beta_t))^2}{\nu(\beta_t)}\right)$	Same as α_3 with a thresholded β on the distance to take into account only close parts of objects.
$F\alpha_2$ - $F\alpha_5$		Fuzzy versions of α_2 - α_5. Objects and β are fuzzy.

6 Experimental Results

The method has been tested with anonymized in-house clinical data. There were acquired in a dental context using 3D cone-beam computed tomography with isotropic voxels, 150 μm long on each dimension. Typical acquired volumes cover the region from the nose bottom to the chin, and from the lips to the temporo-mandibular joint. The main goal is to identify the mandibular canal which is

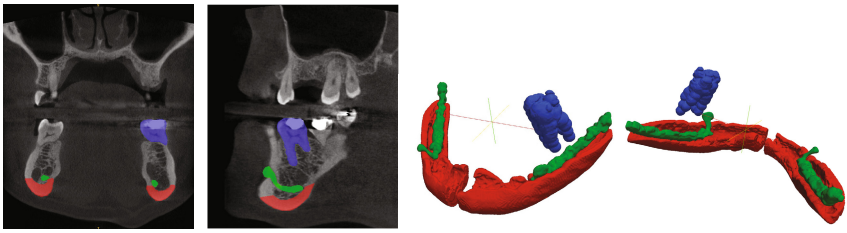

(a) Segmented objects overlayed on a coronal slice. (b) Segmented objects overlayed on a sagittal slice. (c) 3D facial view. (d) 3D dorsal view.

Fig. 2. Manually segmented objects of the maxillofacial area; Mandibular canals are in green, mandibular floors in red and the tooth 36 in blue.

a tubular structure running from the temporo-mandibular joint to the mental foramen through the mandible. An example image is depicted in Figure 2 (a) and (b). This is an original applicative context of spatial relations.

The proposed degrees of alongness have been evaluated on four structures, segmented manually from 3 patients: the left (LMC) and right mandibular canals (RMC), the tooth 36 (the first left-sided mandibular molar in dental classification, noted 36 after) and the left mandibular "floor" (which corresponds to the mandible bottom where the cortical bone is plain, noted LMF, and RMF for the right one, see Figure 2 (c,d)). The alongness degree using each $\alpha_i, i = 1, ..., 5$, is computed for each pair of structures. We expect the highest result between the MF and MC, for each side, as they are two elongated structures in the same direction. Comparing 36 to LMF or LMC should also show significant degrees since the tooth is being along an elongated structure. The other cases should have low degrees. A segmentation example is depicted in Figure 2 (c) and (d). Results can be seen in Figure 3. For the three patients, bar colors differentiate the patient ID (one color each). It can be seen that α_1 shows high degrees for almost all structure pairs except for the left mandibular canal and the floor, which may appear counter intuitive. This can be explained by the distance between structures giving an elongated β as discussed in Section 4.2. As predicted, this version does not fit for our purpose, and is no longer considered. In α_2 results one can observe that the degree is high when comparing the same-sided mandibular canal and the floor, which corresponds well to the intuition, and to a less extent when comparing the tooth to the canal or to the floor, which still makes sense even if the tooth is not an elongated structure. For the other comparisons, the degree is very low (<0.08). This degree appears to differentiate very well the variety of situations. Adding distance information as a distance map does not change much in these cases as α_3 shows a similar profile as α_2. However, using a threshold based on distance seems to be useful. It can be seen in α_4 that taking only the closest parts of the objects could reveal different profiles (e.g. LMF vs 36 for patients 1 and 3). This can be useful for complex-shaped objects

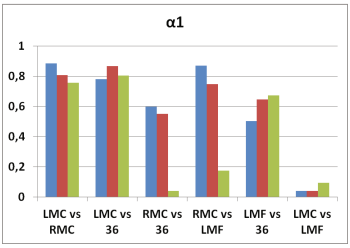

(a) Results for α_1

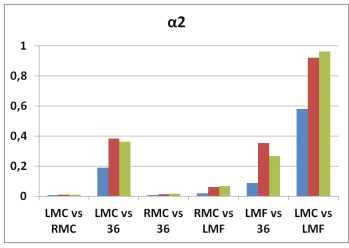

(b) Results for α_2

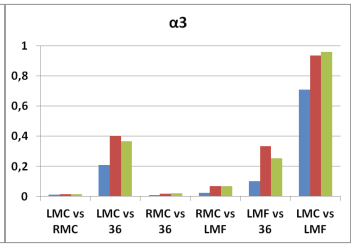

(c) Results for α_3

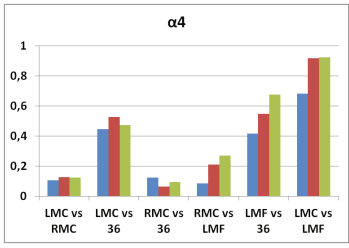

(d) Results for α_4

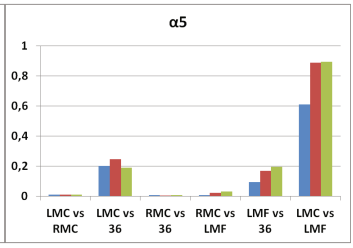

(e) Results for α_5

Fig. 3. Results obtained for crisp objects.

and/or investigating only small parts of objects. Nonetheless this version keeps significant degrees, and we can see that the highest degree is still obtained for the mandibular canal with respect to its mandibular floor. We observe the same behavior with α_5. Thresholds for these tests have been heuristically selected as the median of the distance values range.

Let us now illustrate the fuzzy case. To simulate a fuzzy segmentation of objects, manually segmented structures were considered as the core ($\mu(x) = 1$), and points were added with decreasing membership values from 1 to 0 according to the distance to the core (with 0 at 1.5mm distance). We are interested by fuzziness since it allows us to take into account inter-individual morphology variability, and potential imprecision in the segmentation, which may lead to overlapping structures (which is sometimes the case for MC and MF). Results

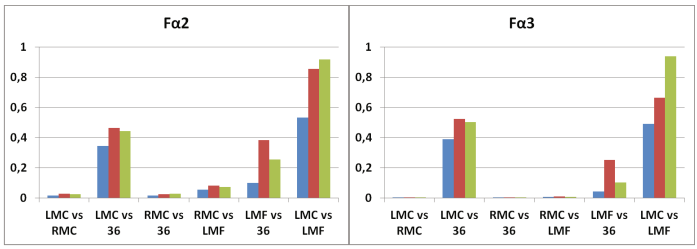

(a) Results for $F\alpha_2$

(b) Results for $F\alpha_3$

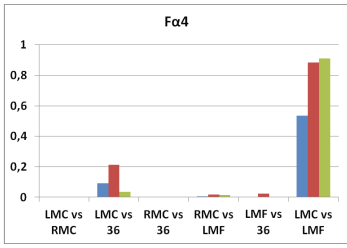

(c) Results for $F\alpha_4$

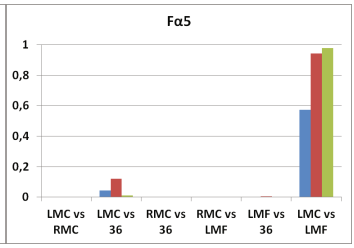

(d) Results for $F\alpha_5$

Fig. 4. Results obtained for fuzzy objects.

using $F\alpha_2$ to $F\alpha_5$ are shown in Figure 4. $F\alpha_2$ displays the same profile as α_2, with the highest degree for the MC/MF case, and quite high degrees for the LMF/36 and LMC/36 cases. Adding distance weighting does not give different results as can be seen with $F\alpha_3$. For $F\alpha_4$ and $F\alpha_5$, using the distance information allows us to pick only close structures and to perform a local analysis. For these tests, the normalizing function for β_t is the same as the one for normalizing the elongation degree (with the parameter a equal to 0.05). Fuzziness allows getting similar degrees when comparing teeth to an elongated structure, while the crisp version is much more sensitive to the tooth position and orientation.

From these results, we decided to select α_2 and $F\alpha_2$ as the best versions, since they are suited for the selected set of objects. Another advantage of selecting these versions is their lower computation cost, since the distance map does not add useful information in our cases. However for other applications, using thresholded versions of β (as α_4) should not be discarded.

The next step was to test the selected version on more data to ensure its robustness. To do so, we included three more patient data, and we also segmented the right mandibular floor to verify the behavior for two elongated structures. The results are summarized in Figure 5.

These results confirm the first tests, sorting correctly the situations depending on their spatial arrangement, and indicating a good robustness with respect to anatomical variability. Hence, we can propose a classification for the degree as follows: between 0 to 0.1 means that the two structures are not linked by an alongness

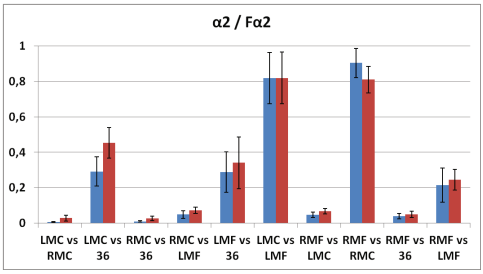

Fig. 5. Mean results obtained for the two selected degrees (α_2 and $F\alpha_2$) on 6 patients. First columns set is α_2 and second is $F\alpha_2$. Standard deviation is shown as error bars

relation, from 0.1 to 0.6 the two structures share a close spatial link with at least one of the structures being elongated, and from 0.6 to 1 the structures can be said to be along each other. Obviously, comparing two degrees inside a same "class" is still meaningful, as a 0.5 degree means higher relationship than a 0.3 degree. In the same way, a 0.58 degree should not be discarded if one look for strong alongness link just because it does not fall into the best "class".

7 Conclusion

In this paper we presented the extension of the "along" spatial relation to 3D, for crisp objects as well as for fuzzy ones, by a two-step process, based on the "between" spatial relation and elongation computation. Several versions are proposed including information such as distance, locality, or object direction, to be able to cope with a wide range of situations, and their performance is tested on clinical cases. Best versions for our precise identification goal are selected for extended tests showing good spatial configuration distinction and a satisfaction degree that can be actually used for comparisons between cases. The measure seems to be robust, but this should be further validated on larger data sets. The measures are invariant by translation and rotation, and most of them by isotropic scaling. The fact that the framework is split into two steps allows easy changes in the methods for computing the inter-objects region or the alongness degree. This paper does not investigate the case of set of disconnected objects which could be meaningful (think of row of trees being along a road for example), since the visibility approach is not designed for, nor the case of very unbalanced object sizes. Maybe the first case could be approached by considering a set of objects as a whole, and looking at its convex hull for example, or by taking a more suited β definition. For the second case, one could make use of the extension of the visibility method, called "myopic vision" and described in [3], which is able to restrain the inter-objects region to the locality of the smallest object. From an application point of view, this work aims to be a tool for automatic segmentation of mandibular canal based on dental cast to help dentists avoiding

post surgery traumas, but could also be applied to other fields like structure identification in geographic information system or vessel-like pattern recognition works. Future work aims to develop other spatial relations representing the maxillofacial region, in order to create a conceptual model, able to guide precise segmentation and recognition, for dental applications.

Acknowledgments. The authors would like to thank the "Association Nationale de la Recherche et de la Technologie" (ANRT) for supporting this research through the CIFRE program.

References

1. Biederman, I.: Recognition-by-components: a theory of human image understanding. Psychological Review **94**(2), 115–147 (1987)
2. Bloch, I.: Fuzzy spatial relationships for image processing and interpretation: a review. Image and Vision Computing **23**(2), 89–110 (2005)
3. Bloch, I., Colliot, O., Cesar, R.M.: On the ternary spatial relation "between". IEEE Transactions on Systems, Man, and Cybernetics **36**(2), 312–327 (2006)
4. Clementini, E.: Qualitative representation of positional information. Artificial Intelligence **95**, 317–356 (1997)
5. Colliot, O., Camara, O., Bloch, I.: Integration of fuzzy spatial relations in deformable models—Application to brain MRI segmentation. Pattern Recognition **39**(8), 1401–1414 (2006)
6. Fouquier, G., Atif, J., Bloch, I.: Sequential model-based segmentation and recognition of image structures driven by visual features and spatial relations. Computer Vision and Image Understanding **116**(1), 146–165 (2012)
7. Freeman, J.: The modelling of spatial relations. Computer Graphics and Image Processing **4**(2), 156–171 (1975)
8. Hayward, W.G., Tarr, M.J.: Spatial language and spatial representation. Cognition **55**, 39–84 (1995)
9. Koenig, O., Reiss, L.P., Kosslyn, S.M.: The development of spatial relation representations: Evidence from studies of cerebral lateralization. Journal of Experimental Child Psychology **50**(1), 119–130 (1990)
10. Montero, R.S., Bribiesca, E.: State of the art of compactness and circularity measures. International Mathematical Forum **4**(27), 1305–1335 (2009)
11. Nempont, O., Atif, J., Bloch, I.: A constraint propagation approach to structural model based image segmentation and recognition. Information Sciences **246**, 1–27 (2013)
12. Rosenfeld, A.: The fuzzy geometry of image subsets. Pattern Recognition Letters **2**(5), 311–317 (1984)
13. Shariff, A., Egenhofer, M.J., Mark, D.M.: Natural-Language Spatial Relations Between Linear and Areal Objects : The Topology and Metric of English. International Journal of Geographical Information Science **12**(3), 215–246 (1998)
14. Takemura, C.M., Cesar, R.M., Bloch, I.: Modeling and measuring the spatial relation "along": Regions, contours and fuzzy sets. Pattern Recognition **45**(2), 757–766 (2012)
15. Vanegas, M.C., Bloch, I., Inglada, J.: Alignment and Parallelism for the Description of High-Resolution Remote Sensing Images. IEEE Transactions on Geoscience and Remote Sensing **51**(6), 3542–3557 (2013)